View metadata, citation and similar papers at core.ac.uk

brought to you by CORE

provided by University of Kentucky

University of Kentucky
UKnowledge

Center for Applied Energy Research Faculty Publications

Center for Applied Energy Research

10-25-2017

Ga and In Modified Ceria as a Support for Cobalt Fischer-Tropsch Synthesis

Muthu Kumaran Gnanamani
University of Kentucky, muthu.gnanamani@uky.edu

Gary Jacobs
University of Kentucky, gary.jacobs@uky.edu

Wilson D. Shafer
University of Kentucky, wilson.shafer@asbury.edu

Michela Martinelli
University of Kentucky, michela.martinelli@uky.edu

Donald C. Cronauer
Argonne National Laboratory

See next page for additional authors

Right click to open a feedback form in a new tab to let us know how this document benefits you.

Follow this and additional works at: https://uknowledge.uky.edu/caer_facpub

Part of the Catalysis and Reaction Engineering Commons

Repository Citation

Gnanamani, Muthu Kumaran; Jacobs, Gary; Shafer, Wilson D.; Martinelli, Michela; Cronauer, Donald C.; Kropf, A. Jeremy; Marshall, Christopher L.; and Davis, Burtron H., "Ga and In Modified Ceria as a Support for Cobalt Fischer-Tropsch Synthesis" (2017). *Center for Applied Energy Research Faculty Publications*. 25.
https://uknowledge.uky.edu/caer_facpub/25

This Article is brought to you for free and open access by the Center for Applied Energy Research at UKnowledge. It has been accepted for inclusion in Center for Applied Energy Research Faculty Publications by an authorized administrator of UKnowledge. For more information, please contact UKnowledge@lsv.uky.edu.

Authors
Muthu Kumaran Gnanamani, Gary Jacobs, Wilson D. Shafer, Michela Martinelli, Donald C. Cronauer, A. Jeremy Kropf, Christopher L. Marshall, and Burtron H. Davis

Ga and In Modified Ceria as a Support for Cobalt Fischer-Tropsch Synthesis

Notes/Citation Information
Published in *Applied Catalysis A: General*, v. 547, p. 115-123.

© 2017 Elsevier B.V. All rights reserved.

This manuscript version is made available under the CC-BY-NC-ND 4.0 license
https://creativecommons.org/licenses/by-nc-nd/4.0/.

The document available for download is the author's post-peer-review final draft of the article.

Digital Object Identifier (DOI)
https://doi.org/10.1016/j.apcata.2017.08.026

This article is available at UKnowledge: https://uknowledge.uky.edu/caer_facpub/25

Ga and In modified Ceria as a support for Cobalt Fischer-Tropsch Synthesis

Muthu Kumaran Gnanamani[1], Gary Jacobs[1,2], Wilson D. Shafer[1], Michela Martinelli[1], Donald C. Cronauer[3], A. Jeremy Kropf[3], Christopher L. Marshall[3], Burtron H. Davis[1*]

[1]*Center for Applied Energy Research, University of Kentucky, 2540 Research Park Drive, Lexington, Kentucky 40511, USA*

[2] *University of Texas at San Antonio, Department of Biomedical and Chemical Engineering, UTSA Circle, San Antonio, TX 78249*

[3]*Chemical Sciences and Engineering Division, Argonne National Laboratory, Argonne, IL, 60439, USA*

Abstract

Ceria modified by the addition of gallium or indium (20 mol%) was used as a support for cobalt Fischer-Tropsch synthesis. The addition of gallium to ceria improved the CO conversion for cobalt, whereas indium tended to decrease it. A similar trend was observed with the Ag-promoted cobalt/ceria catalysts that were doped with Ga or In. For Ag promoted catalysts, doping with Ga or In decreased methane and increased the product selectivities of olefins and alcohols. The sum of olefins and alcohols in terms of product selectivity for the Ag-promoted catalysts decreased in the following order: Ag-Co/Ce-Ga > Ag-Co/Ce-In > Ag-Co/Ce. The H_2-TPR-XANES data shown that addition of gallium or indium to ceria increased the fraction of surface Ce^{3+} for both unpromoted and Ag promoted catalysts. This partially reduced ceria plays an important role in the product selectivity of cobalt for FT synthesis.

Keywords: Fischer-Tropsch synthesis; Ag promoter; CeO_2; CeO_2-Ga_2O_3; CeO_2-In_2O_3; oxygenates

*Corresponding author. Tel.: +1-859-257-0251; email address: burtron.davis@uky.edu

1.0 Introduction

The Fischer-Tropsch synthesis (FTS) is an attractive process used to convert syngas derived from coal, biomass, and natural gas to clean transportation fuels and chemicals [1-4]. Cobalt and iron are the two elements most used as catalysts by industry [5-8]. The cobalt-based FT catalysts are often used to produce long straight-chain hydrocarbons with minimal olefin and oxygenate contents. On the other hand, iron catalysts produce a significant amount of olefins and oxygenates along with n-alkanes. This difference in FT selectivity between iron and cobalt is generally explained by the nature of active sites and their adsorption behavior of CO and H_2 as well as the influence of reaction conditions [9-12]. The active form of cobalt in FT synthesis is metallic in nature [13], whereas for iron it is the iron carbide [14]. Due to intrinsic water-gas shift activity, the Fe-FT catalyst can be operated at a relatively low H_2/CO ratio (~1.0) in comparison with cobalt catalyst which requires a H_2/CO ratio of ~2.0 [14].

Many factors affect the FT activity and the product selectivity of cobalt catalysts. In this regard, the support plays a vital role in controlling cobalt metal dispersion through the metal-support interaction [15-18]. Promoters such as Pt, Ag, Pd, Ru, and Re [19-23] were added along with cobalt on to the support in order to increase the fraction of reduced cobalt nanoparticles after activation in H_2. In general, supports like Al_2O_3, SiO_2, TiO_2, ZrO_2, and zeolites [24-28] are commonly used. Very recently partially reducible oxides such as CeO_2 also showed promising results as a support for cobalt FT synthesis [29-31]. Ceria is a versatile oxide that can generate oxygen vacancies under reducing conditions. In many instances, oxygen vacancies serve as adsorption sites for reactants (e.g., water-shift reaction [32], dehydration [33]). On the other hand, the metal-support interface is also very important in the sense that the intermediates formed on the

metal surface can interact with another adsorbate at the metal-metal oxide interface to yield different products [34].

In our earlier investigations, cobalt supported on CeO_2 [30] and higher rare earth oxide (REO) modified CeO_2 [31] catalysts were shown to have higher selectivity for alcohols in comparison with a conventional alumina supported cobalt catalyst. We offered an explanation that the selectivity control is achieved by terminating the FT growth either through the addition of mobile bridging OH groups located on ceria or through termination by molecular CO from surface species (e.g., formates formed from the reaction of CO with bridging OH groups) located on ceria. We concluded that the metal-support interface of supported cobalt catalysts may be involved in the synthesis of alcohols. Johnston and Joyner [34] observed for the first time the possible nucleophilic attack by adsorbed hydroxyl groups in oxygenates synthesis from syngas, and indicated the existence of common intermediates to both oxygenate and hydrocarbon synthesis, possibly through an adsorbed ethylidyne species. On the other hand, the Baker group [35] claimed that the unreduced cobalt ions were responsible for producing a significant amount of higher oxygenates using silica supported Co-Cu bimetallic catalysts.

In the present investigation, we have studied the effect of gallium or indium additions on the reducibility of ceria by using the H_2-TPR XANES technique. The dispersion of cobalt particles on ceria modified supports was evaluated by using the HRTEM technique. Both cobalt and Ag-promoted cobalt catalysts supported on ceria, Ga- and In-modified ceria were tested for Fischer-Tropsch synthesis using a 1L CSTR. The aim was to assess the reducibility of ceria and their interrelations with activity and the product selectivity of cobalt for FT synthesis.

2.0 Experimental

2.1 Catalyst preparation

The supports, ceria and Ga- and In-modified ceria were prepared by following the homogeneous precipitation method using urea decomposition. In this method, an appropriate amount of $Ce(NO_3)_3.6H_2O$ (Alfa Aesar, 99.5%) and $Ga(NO_3)_3.xH_2O$ (Alfa Aesar, 99%) or $In(NO_3)_2.xH_2O$ with Ce and Ga or Ce and In molar ratios of 80:20 were first dissolved simultaneously in deionized water at room temperature (~25°). In a separate beaker, the required quantity of urea (usually ~4 times that of the molar equivalent of metal nitrates) was dissolved in deionized water and then mixed with the metal nitrates solution. The resulting solution was refluxed at 85-90°C with constant stirring (500 rpm) for 15 h. The precipitate obtained was filtered and washed three times using deionized water. It was then dried in a static air oven at 120°C and calcined in air in a muffle furnace at 500°C for 3 h. To the supports, 5 wt% Co with and without Ag (0.55 wt%) were added by sequential incipient wetness impregnation (Co-first), followed by drying and calcining at 350°C for 3 h. Hereafter, the catalysts will be referred as Co/Ce, Co/Ce-Ga, Co/Ce-In, Ag-Co/Ce, Ag-Co/Ce-Ga, and Ag-Co/Ce-In.

2.2 Catalyst characterization

BET surface area and porosity characteristics of the calcined catalysts were measured using a Micromeritics 3-Flex system. Before performing the test, the temperature was gradually ramped to 160 °C and the sample was evacuated at this temperature for 12 h to approximately 50 mTorr. The BET surface area, single point pore volume, and single point average pore diameter were obtained. The Barrett-Joyner-Halenda (BJH) method was also used to estimate pore volume and average pore diameter, as well as to provide pore size distribution as a function of pore radius.

In-situ H_2-TPR XAFS studies were performed at the Materials Research Collaborative Access Team (MR-CAT) beamline at the Advanced Photon Source, Argonne National Laboratory. A cryogenically cooled Si(1 1 1) monochromator was used to select the incident energy and a

rhodium-coated mirror was used to reject higher order harmonics of the fundamental beam energy. The experiment setup was as outlined by Jacoby [36]. A stainless steel multi-sample holder (4.0 mm i.d. channels) allowed for testing the in-situ reduction of six samples during temperature programmed heating. Catalyst samples were diluted with silica gel at a weight ratio (silica/sample) of approximately 12. Approximately 5 mg of each sample was loaded as a self-supporting wafer in each channel. The holder was placed in the center of a quartz tube, equipped with gas and thermocouple ports and Kapton windows. The amount of sample used was optimized for the Ce L_{III} edge (5723 eV). The quartz tube was placed in a clamshell furnace mounted on a positioning table. Each sample cell was positioned relative to the beam by finely adjusting the position of the table to an accuracy of 20 μm for repeated scans. Once the sample positions were fine-tuned, the reactor was purged with helium for more than 5 min at 30 ml/min. Then, the reactant gas (H_2/He, 3.5%) was flowed through the samples (95 ml/min) and a temperature ramp of ~1.2 ^oC/min was initiated for the furnace. The final temperature was ~875^oC.

The Ce L_{III}-edge spectra were recorded in transmission mode and a Cr metallic foil spectrum was measured simultaneously with each sample spectrum for energy calibration. X-ray absorption spectra for each sample were collected from 5575 to 6136 eV, with a step size of: from -150 to -35 eV, 10 eV; from -35 eV to -15 eV, 3 eV; from -15 to 25 eV, 0.7 eV; from 25 eV to 35 eV, 1 eV; and from 35 eV to 10.4k, 0.08k. The acquisition time was ~4.5 min per spectrum. By measuring each sample, in turn, and repeating, this allowed for approximately 25 scans to be collected for each sample over ~11 h. A sample's temperature change from the absorption edge through the end of the scan was then about 18 ^oC, while a spectrum was measured approximately every 33 ^oC. Data reduction of the XAFS spectra was carried out using the WinXAS program [37], and raw data were processed to give the normalized XANES spectra. Linear combination

fitting of spectra with appropriate reference compounds was carried out. The initial spectrum of each catalyst was used as a fingerprint for the Ce^{4+} oxidation state, while the final spectrum of a 0.5%Pt/$Ca_{0.50}Ce_{0.50}O_X$ catalyst following TPR (30 ml/min of 4%H_2/He, 820ºC, 1.5 h hold time) from [38] was used as a fingerprint of the Ce^{3+} oxidation state for all samples, since its lineshape resembled Ce^{3+} compounds, such as $Ce(NO_3)_3$ or $Ce(Cl_3)_3$. EXAFS data reduction and fitting were carried out using the WinXAS program [37], Atoms [39], FEFF [40] and FEFFIT [41] programs. The k- and r-ranges were chosen to be approximately 2.5–10 $Å^{-1}$ and 1.1–3.2 Å, respectively.

Transmission electron microscopy (TEM) imaging was performed using a JEOL 2010F field-emission gun TEM with an accelerating voltage of 200 keV and magnification ranging from 50 to 1000 K. High-resolution imaging was performed using a symmetrical multibeam illumination with a beam resolution of 0.5 nm. Images were recorded using a Gatan Ultrascan 4k × 4k CCD camera, and data were analyzed using Gatan Digital Micrograph software.

2.3 *Fischer-Tropsch synthesis*

Fischer–Tropsch synthesis was performed using a 1 L CSTR. Typically, 15.0 g of calcined catalyst (60-100 microns) was reduced *ex-situ* using a H_2:He (1:3) mixture at 350°C for 20 h. The pre-reduced catalyst was transferred to a 1 L CSTR which already contained 310 g of melted Polywax 3000 (polyethylene having an average carbon number of 200) under flowing nitrogen. The catalyst then subjected to H_2 polishing with pure H_2 (30 slph) at 230°C for 24 h. The FT synthesis was performed at a temperature of 220°C and a syngas pressure of 1.99 MPa at a constant H_2/CO feed of 2. The effluent gases were analyzed online using a Micro GC (HP, Quad series, Refinery Gas analyzer) equipped with a TCD detector, while the liquid products condensed in the 0° and 100° traps were analyzed separately using an HP 6890 GC with DB-5 capillary column. The aqueous product mixture was analyzed by using SRI-GC (model no. 8610C) with TCD

detector and Porapak Q packed column. The conversion and selectivity reaction parameters are defined as:

$$conversion = \ 100\ x \frac{n_{CO\ in} - n_{CO_{out}}}{n_{CO\ in}}$$

$$selectivity = 100\ x \frac{n_{product_{out}}.\ carbon\ number}{n_{CO\ in} - n_{CO\ out}}$$

where $n_{CO\ in}\ and\ \ n_{CO\ out}$ are the number of moles of CO fed and not-consumed, respectively. The selectivity is defined as the percent mole of CO consumed to form a particular C_n product (hydrocarbon, CO_2 or oxygenate), normalized by the amount of CO consumed.

3.0 Results and discussion

Figure 1 shows the CO conversion for the unpromoted (left) and Ag-promoted (right) cobalt. The Co/Ce and Co/Ce-Ga catalysts both displayed CO conversions at about 17%. The Co/Ce-Ga catalyst exhibited a relatively less deactivation with time-on-stream compared to Co/Ce while Co/Ce-In displayed CO conversions of only about 6%. The promotional effect of Ag on the CO conversion is noted only for Ce-Ga and Ce-In supported cobalt catalysts. Co/Ce-Ga and Ag-Co/Ce-Ga catalysts outperformed Ce and Ce-In supported cobalt catalysts for CO conversions.

The product selectivity to methane for unpromoted and Ag-promoted cobalt catalysts are shown in **Figure 2**. The addition of Ga or In tended to decrease the selectivity of methane for cobalt and they followed the decreasing trend Co/Ce > Co/Ce-Ga > Co/Ce-In irrespective of whether Ag promoter was present or not. **Figure 3** shows that the selectivity to CO_2 for Co/Ce and Co/Ce-Ga catalysts remained more or less the same at about 4% while with Co/Ce-In the CO_2 selectivity was significantly higher (~6.5%). A similar trend in the selectivity to CO_2 is observed with Ag-promoted catalysts as that of the unpromoted counterparts. The higher CO_2 selectivity has been reported in our previous work using ceria supported cobalt catalysts [30,31].

It is interesting to see if any changes occurred in the product distribution of olefins and alcohols with the addition of Ga or In on to CeO_2. For this purpose, the total olefin and alcohol products formed during FT synthesis was summed and compared among all the three Ag-promoted catalysts at various times-on-stream (**Figure 4**). The Ag-Co/Ce-Ga catalyst showed a significantly higher selectivity for olefin and alcohol at about 30% in comparison with Ag-Co/Ce and Ag-Co/Ce-In catalysts, which showed only about 20%. It is also noted that the sum of olefins and alcohols selectivity for all the three catalysts increased with increasing time-on-stream. Ribeiro et al. [31] observed such an increasing trend in alcohols selectivity with reaction time for cobalt. The authors explained this behavior based on HRTEM and XANES analyses of the used catalysts in that the metallic character of cobalt was partly transformed into cobalt carbide which could possibly influence alcohol and CO_2 formation from syngas. Hence, we cannot rule out this possibility in the present system.

The lower olefins are important raw materials for the petrochemical industry. In this regard, we made a comparison graph of C_2-C_4 olefins selectivity with time-on-stream for the three Ag-promoted Co/Ce catalysts as shown in **Figure 5**. The olefins selectivity ranged from 8 to 10%, from 12 to 14%, and from 5 to 8% for Ag-Co/Ce, Ag-Co/Ce-Ga, and Ag-Co/Ce-In catalysts, respectively. Overall, the olefinic content decreased with increasing time.

Table 1 displays the results of nitrogen physisorption at 77 K. The BET surface area of the starting support materials Ce, Ce-Ga, and Ce-In were 90, 104, and 79 m^2/g, respectively. After impregnation of cobalt (5 wt%), the BET surface area of the support decreased to 71, 84, and 61 m^2/g for Ce, Ce-Ga, and Ce-In, respectively. If the Co_3O_4 does not contribute significantly to the surface area, then assuming that 5%Co corresponds to 6.75%Co_3O_4, the expected decrease would be to 83.9 m^2/g for Co/Ce, 97 m^2/g for Co/Ce-Ga, and 74 m^2/g for Co/Ce-In catalysts. Since we

obtained slightly lower values for all three catalysts, this indicates that some minor pore blocking occurred. However, further addition of 0.55 wt% Ag did not change the surface area of Co/Ce (Ce, Ce-Ga, Ce-In) appreciably. The single point pore volume as well as the BJH pore volume (desorption) of the catalysts also followed a similar trend to that of the BET surface area. The BJH pore size distributions of unpromoted as well as Ag-promoted Co/Ce (Ce, Ce-Ga, Ce-In) catalysts are shown in **Figure 6**. The distributions remained narrow for all the catalysts indicating that cobalt particles do not significantly alter the porous structure of the support.

To better interpret the standard TPR profiles, TPR-XANES experiments at the Ce L_{III} edge (5723 eV) were carried out using H_2. The XANES lineshapes of Ce^{3+} and Ce^{4+} oxidation states exhibit distinct differences, as shown in **Figure S1**, where spectra of reference compounds as described in the experimental section are provided. The high energy XANES peak (often denoted Peak C) for Ce^{4+} is typically assigned to absorption into the 5d level with no occupancy in 4f for either the initial or final state, and is present in completely oxidized CeO_2, but absent for Ce^{3+} (final state configuration: Ce $[2p^5 4f^{\ 0} 5d^1]$ O $[2p^6]$). With surface shell reduction, the high energy peak decreases; further decreases are observed upon reduction of the bulk at higher temperature. The low energy peak (labeled B) is split into at least two separate assignments [42, 43]. Peak B_1, also present in CeO_2 with Ce^{4+}, has been assigned to absorption into the 4f level in the final state. Thus, in addition to the excitation of an electron from the Ce 2p shell to the 5d shell, another excitation occurs, coming from the valence band (O 2p shell) to the Ce 4f shell, leaving a hole in the valence band (final state configuration Ce $[2p^5 4f^{\ 1} 5d^1]$ O $[2p^5]$). As the reduction of Ce occurs, peaks B_1 and C diminish and a new peak, B_0, develops as a shoulder. Located just below peak B_1, B_0 is associated with absorption into the 5d level, with 4f occupancy in the initial state (final state configuration Ce $[2p^5 4f^{\ 1} 5d^1]$ O $[2p^6]$). The intensity of B_0 first increases with surface shell

reduction of ceria, and then again with bulk Ce reduction. Using these lineshape differences as a guide, the degree of reduction of ceria was estimated by linear combination fitting of XANES spectra with Ce^{3+} and Ce^{4+} reference compounds using WinXAS [37]. In **Figure 7**, each TPR begins with ceria being present as Ce^{4+}. Both the lower temperature surface shell reduction and higher temperature bulk reduction are easily observed for the six catalysts. Extents of reduction as quantified by LC fittings in **Figure 8** show that doping Ce with In or Ga improves the extent of surface shell reduction from ~10% as Ce^{3+} for the undoped Co/Ce and Ag-Co/Ce catalysts, to ~15% with In-doping and 20% with Ga-doping at the 20% level. Ag promoter, on the other hand, tends to facilitate surface shell reduction, shifting the temperature of surface shell reduction from ~300^{o}C to a lower temperature below 250^{o}C, perhaps by a H_2 dissociation and spillover mechanism. A comparison at 235^{o}C is provided as **Figure S2** to highlight the line shape differences. Reduction of ceria may occur by converting surface capping O to OH, or by generating surface O vacancies [44].

To highlight the effect of In and Ga doping of ceria on Ce-O coordination, EXAFS fittings were conducted on spectra recorded at the initial condition and at 235^{o}C, as shown in **Figure S3**, **S4**, and **S5** for the undoped, Ga-doped, and In-doped catalysts, respectively. **Table 2** summarizes the results of fitting the first shell of Ce-O coordination. Using the initial spectrum as a basis, the changes in Ce-O coordination are not significant for the catalysts without Ag promoter, but indicate that surface shell reduction of Ce has occurred for the catalysts containing the Ag promoter. Moreover, the decreases in Ce-O coordination are somewhat higher for the catalysts containing Ga and In. Note, however, that the uncertainties are quite high. Thus, the results only lend support to the conclusions obtained from XANES spectroscopy.

The HR-TEM images of the reduced sample of Ag-Co/Ce, Ag-Co/Ce-Ga, and Ag-Co/Ce-In are shown in **Figure 9**. In the reduced Ag-Co/Ce catalyst (9A), the magnified image shows (right) uniformly distributed cobalt particles and the particle sizes of cobalt ranged between 5 and 8 nm. The reduced sample of Ag-Co/Ce-Ga (9B) and Ag-Co/Ce-In (9C) contain cobalt particles just located at the edges of Ce-Ga or Ce-In particles. The EDS performed over the circled region as shown in **Figure 9** indicates that the particles are indeed cobalt. The data reveal that the dispersion of cobalt on these supports remained more or less the same.

The mechanism of oxygenates formation in Fischer-Tropsch synthesis has been under scrutiny for many years [45]. In cobalt-based FT synthesis, the amount of oxygenates formed typically varies from 1 to 3 mol% whereas Fe produced a considerable amount of oxygenates typically between 5 and 30 mol% or above depending on the synthesis conditions and the presence of alkali promoters. Linear alcohols are the primary oxygenate products found in both Fe- and Co-based FT synthesis. Many argue that CO insertion across a metal-R (R=alkyl, alkenyl) bond is the plausible route to the formation of alcohols from syngas using a Fe or Co catalyst. However, the adsorbed hydroxyl groups on partially reducible oxides such as lanthanides could also be involved in the formation of alcohols by nucleophilic addition. Our previous studies indicated that ceria enhanced the formation of alcohols from syngas under a typical FT synthesis conditions; moreover, the particle size of cobalt as well as the partially reduced nature of the cerium oxide both played a vital role in controlling FT product selectivity [30,31].

In general, Co metal sites are responsible for the FT chain growth. The metal-oxide support interface could act as a termination site for the FT synthesis where hydroxyl groups or molecular CO (e.g., from formate, etc.) on the oxide support may be involved in chain termination. Therefore, it is desired to have more metal-support interface to promote alcohol formation from

syngas. In this regard, we have made an attempt to promote the surface reduction of ceria (i.e., increasing the number of bridging OH groups associated with oxygen vacancies) by doping ceria with Ga or In. We found that the addition of Ga or In to Co/Ce increased the partial reduction of surface ceria as evidenced from H_2-TPR XANES in which the Ce^{3+} concentration was relatively higher in the case of Co/Ce-Ga and Co/Ce-In catalysts compared to Co/Ce at a given temperature. The same trend was observed using the Ag-promoted catalysts. The selectivity to oxygenates for Co/Ce-Ga and Co/Ce-In catalysts followed a similar trend as the extent of reduction of the support. After 160 h of time-on-stream, the sum of oxygenates and olefins selectivity was about 30% for Ag-Co/Ce-Ga, whereas Ag-Co/Ce and Ag-Co/Ce-In catalysts both only showed about 20%. This difference in the selectivity observed between Ag-Co/Ce and Ag-Co/Ce-Ga or Ag-Co/Ce-In could be due to the presence of more partially reduced ceria in the case of Ag-Co/Ce-Ga catalyst after activation in H_2 as inferred by the H_2-TPR XANES studies.

4.0 Conclusions

CeO_2, CeO_2-Ga_2O_3, and CeO_2-In_2O_3 were prepared by following the homogeneous precipitation method using urea decomposition and used as supports for cobalt FT synthesis. The addition of Ga or In was found to increase the BET surface area and the pore volume of the support. The H_2-TPR XANES data indicate that Ga or In addition tended to increase the surface partial reduction of ceria. The HR-TEM analyses on the reduced catalysts indicate that the distribution of cobalt particle sizes remained the same for all the supports. The addition of Ga was found to decrease methane formation and increase olefins and oxygenates selectivity for cobalt. However, the promotional effect by addition of indium to Co/CeO_2 or Ag-Co/CeO_2 is marginal. The increase in metal-oxide support interface is key to the production of olefins and alcohols for cobalt FT catalysts using ceria.

Acknowledgements

The work carried out at the CAER was supported in part by funding from the Commonwealth of Kentucky. Argonne's research was supported in part by the U.S. Department of Energy (DOE), Office of Fossil Energy, National Energy Technology Laboratory (NETL). The use of the Advanced Photon Source was supported by the U.S. Department of Energy, Office of Science, Office of Basic Energy Sciences, under Contract No. DE-AC02-06CH11357. MRCAT operations are supported by the Department of Energy and the MRCAT member institutions.

References

1. M.E. Dry, Appl. Catal. A: Gen. 138 (1996) 319-344.
2. H.H. Storch, N. Golumbic, R.B. Anderson, The Fischer-Tropsch and Related Synthesis, Wiley, New York, 1951.
3. D. Chakrabarti, V. Prasad, A. de Klerk, "Mechanism of the Fischer-Tropsch Process" in Fischer-Tropsch Synthesis, Catalysts, and Catalysis Advances and Applications, Chem. Indus. Edited by B.H. Davis and M.L. Occelli (2016) pages 183-222.
4. G. Jacobs, W. Ma, B.H. Davis, Catalysts 4 (2014) 49-76.
5. E. Rytter and A. Holmen, Catalysts 5 (2015) 178-499.
6. H. Jahangiri, J. Bennett, P. Mahjoubi, K. Wilson, S. Gu, Catal. Sci. Technol. 4 (2014) 2210-2229.
7. A.Y. Khodakov, W. Chu, P. Fongarland, Chem. Rev. 107(5) (2007) 1692-1744.
8. E. de Smit and B.M. Weckhuysen, Chem. Soc. Rev. 37 (2008) 2758-2781.
9. B.H. Davis, Ind. Eng. Chem. Res. 46(26) (2007) 8938-8945.
10. H. Schulz, E. vein Steen, M. Claeys, Stud. Surf. Sci. Catal. 81 (1994) 455-460.
11. F.G. Botes, H. Niemantsverdriet, J. van de Loosdrecht, Catal. Today 215 (2013) 112-120.
12. W. Desheng and G. Naijia, Journal of Natural Gas Chemistry 9(3) (2000) 249-262.
13. J.C. Mohandas, M.K. Gnanamani, G. Jacobs, W. Ma, Y. Ji, S. Khalid, B.H. Davis, ACS Catal. 1(11) (2011) 1581-1588.
14. J.F. Shultz, W.K. Hall, B. Seligman, R.B. Anderson, J. Am. Chem. Soc. 77(1) (1955) 213-221.
15. Ø. Borg, P.D.C. Dietzel, A.I. Spjelkavik, E.Z. Tveten, J.C. Walmsley, S. Diplas, S. Eri, A. Holmen, E. Rytter, J. Catal. 259(2) (2008) 161-164.

16. G. Jacobs, T.K. Das, Y. Zhang, J. Li, G. Racoillet, B.H. Davis, Appl. Catal. A: Gen. 233(1-2) (2002) 263-281.

17. E. Iglesia, Appl. Catal. A: Gen. 161 (1997) 59-78.

18. M.K. Gnanamani, G. Jacobs, U.M. Graham. W. Ma, V.R.R. Pendyala, M. Ribeiro, B.H. Davis, Catal. Lett. 134(1) (2010) 37-44.

19. K. Keyvanloo, M.J. Fisher, W.C. Hecker, R.J. Lancee, G. Jacobs, C.H. Bartholomew, J. Catal. 327 (2015) 33-47.

20. D.J. Moodley, J. van de Loosdrecht, A.M. Saib, M.J. Saib, M.J. Overett, A.K. Datye, J.W. Niemantsverdriet, Appl. Catal. A: Gen. 354 (2009) 102-110.

21. G. Jacobs, J.A. Chaney, P.M. Patterson, T.K. Das, B.H. Davis, Appl. Catal. A: Gen. 264 (2004) 203-212.

22. G. Jacobs, J.A. Chaney, P.M. Patterson, T.K. Das, J.C. Maillot, B.H. Davis, J. Synch. Rad 11 (2004) 414-422.

23. T. Jermwongratanachai, G. Jacobs, W. Ma, W.D. Shafer, M.K. Gnanamani, P. Gao, B. Kitiyanan, B.H. Davis, J.L.S. Klettlinger, C.H. Yen, D.C. Cronauer, A.J. Kropf, C.L. Marshall, Appl. Catal. A: Gen. 464-465 (2013) 165-180.

24. K. Shimura, T. Miyazawa, T. Hanaoka, S. Hirata, Appl. Catal. A: Gen. 494 (2015) 1-11.

25. M.K. Gnanamani, G. Jacobs, V.R.R. Pendyala, U. M. Graham, S.D. Hopps, G.A. Thomas, W.D. Shafer, D.E. Sparks, Q. Xiao, Y. Hu, B.H. Davis, Appl. Catal. A: Gen. 523 (2016) 146-158.

26. K. Shimura, T. Miyazawa, T. Hanaoka, S. Hirata, Appl. Catal. A: Gen. 460-461 (2013) 8-14.

27. P.A. Chernavskii, A.S. Lermontov, G.V. Pankina, S.N. Torbin, V.V. Lunin, Kinetics and Catalysis, 43(2) (2002) 268-274.

28. S. Bessell, Appl. Catal. A: Gen. 126(2) (1995) 235-244.

29. M.K. Gnanamani, M.C. Ribeiro, W. Ma, W.D. Shafer, G. Jacobs, U.M. Graham, B.H. Davis, Appl. Catal. A: Gen. 393(1-2) (2011) 17-23.

30. M.K. Gnanamani, G. Jacobs, U.M. Graham, M.C. Ribeiro, F.B. Noronha, W.D. Shafer, B.H. Davis, Catal. Today 261 (2016) 40-47.

31. M.C. Ribeiro, M.K. Gnanamani, K.R. Azevedo, R.C.R.-Neto, V.R.R. Pendyala, G. Jacobs, B.H. Davis, F.B. Noronha, Topics in Catal. 57(6) (2014) 550-560.

32. G. Jacobs, L. Williams, U. Graham, G.A. Thomas, D.E. Sparks, B.H. Davis, Appl. Catal. A: Gen. 252 (2003) 107-118.

33. M.K. Gnanamani, G. Jacobs, W.D. Shafer, B.H. Davis, ChemCatChem 9 (2017) 492-498.

34. Johnston and R.W. Joyner, Stud. Surf. Sci. Catal. 75 (1993) 165-180.

35. J.E. Baker, R. Burch, S.J. Hibble, P.K. Loader, Appl. Catal. 65 (1990) 281-292.

36. M. Jacoby, Chem. Eng. News 79 (32) (2001) 33-38.

37. T. Ressler, J. Syn. Rad. 5 (1998) 118-122.

38. L.Z. Linganiso, G. Jacobs, K.G. Azzam, U.M. Graham, B.H. Davis, D.C. Cronauer, A.J. Kropf, C.L. Marshall, Appl. Catal. A: Gen. 394 (2011) 105-116.

39. B. Ravel, "ATOMS: crystallography for the x-ray absorption spectroscopist," J. Syn. Rad. 8 (2001) 314-316.

40. J.J. Rehr, R.C. Albers, Rev. Modern Phys. 72 (2000) 621-654.

41. M. Newville, B. Ravel, D. Haskel, E.A. Stern, Y. Yacoby, Physica B 208-209 (2005) 154-156.

42. S.H. Overbury, D.R. Huntley, D.R. Mullins, G.N. Glavee, Catal. Lett. 51 (1998) 133-138.

43. J. El Fallah, S. Boujani, H. Dexpert, A. Kiennemann, J. Majerus, O. Touret, F. Villain, F. Le Normand, J. Phys. Chem. 98 (1994) 5522-5533.

44. G. Jacobs, U.M. Graham, E. Chenu, P.M. Patterson, A. Dozier, B.H. Davis, J. Catal. 229 (2005) 499-512.

45. R.A. van Santen. M. Ghouri, E.M.J. Hensen, Phys. Chem. Chem. Phys. 16 (2014) 10041-10058.

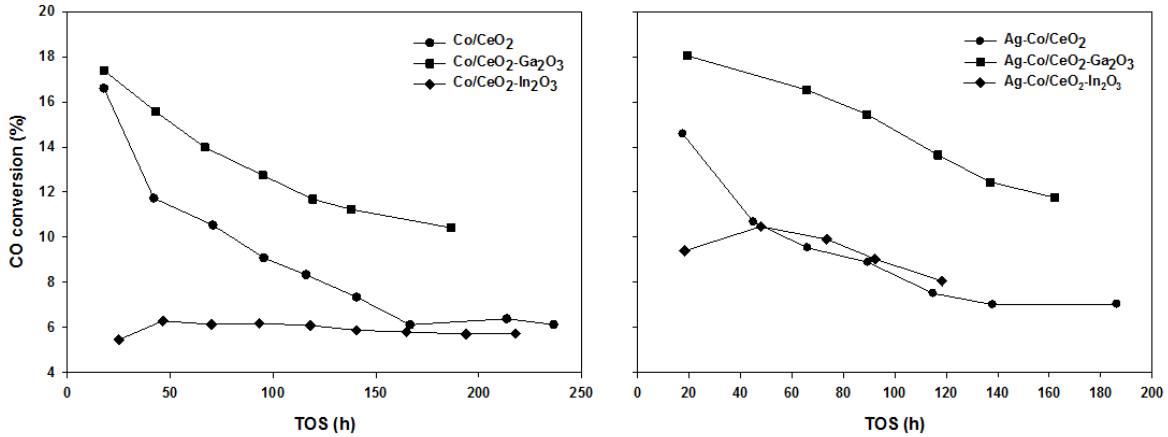

Figure 1. CO conversion over the unpromoted (left) and Ag-promoted (right) Co/Ce (Ce, Ce-Ga, Ce-In) catalysts. (Reaction condition: T=220°C, P=300 psig, H_2/CO=2.0, SV=0.75 nL/h/g cat.).

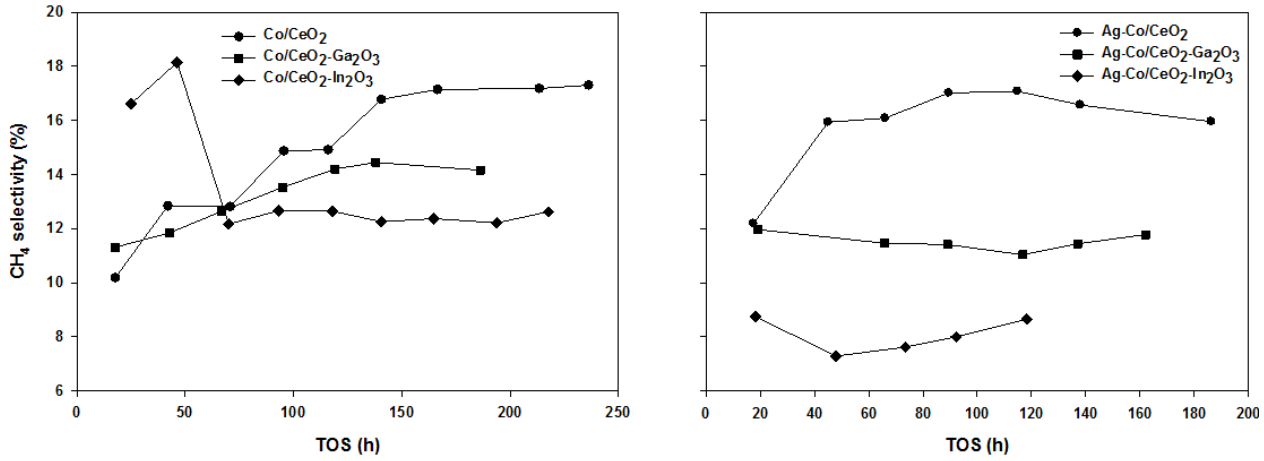

Figure 2. Methane selectivity as a function of time on-stream for FT synthesis over the unpromoted (left) and Ag-promoted (right) Co/Ce (Ce, Ce-Ga, Ce-In) catalysts. (Reaction condition: T=220°C, P=300 psig, H_2/CO=2.0, SV=0.75 nL/h/g cat.).

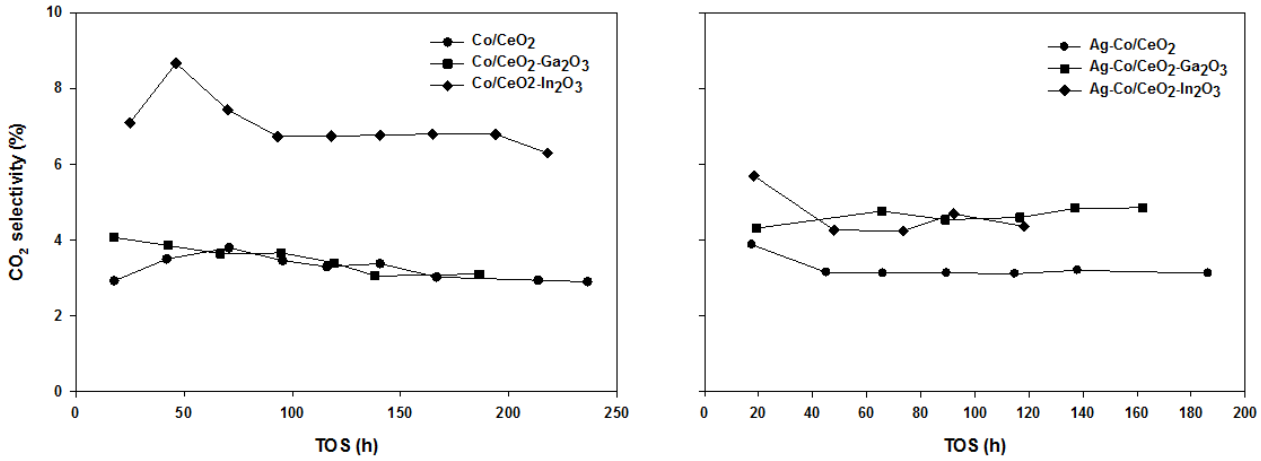

Figure 3. CO_2 selectivity as a function of time on-stream for FT synthesis over the unpromoted (left) and Ag-promoted (right) Co/Ce (Ce, Ce-Ga, Ce-In) catalysts. (Reaction condition: T=220°C, P=300 psig, H_2/CO=2.0, SV=0.75 nL/h/g cat.).

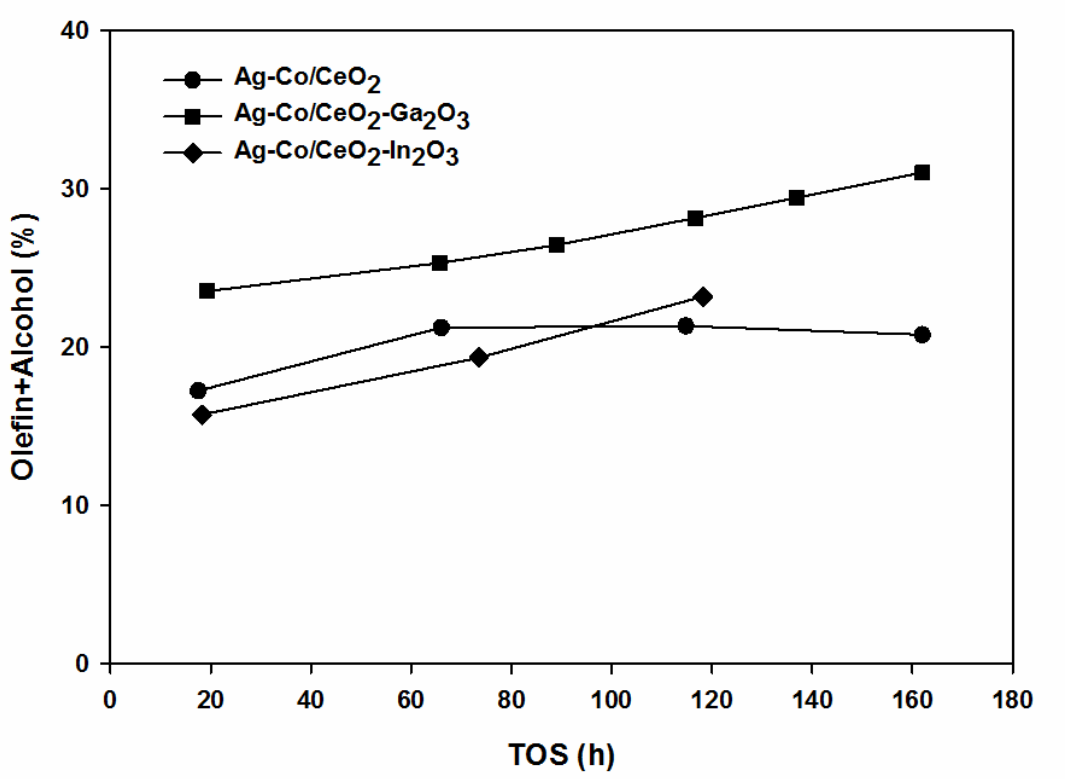

Figure 4. The sum of olefins and alcohol products selectivity as a function of time on-stream for FT synthesis over the Ag-promoted Co/Ce (Ce, Ce-Ga, Ce-In) catalysts. (Reaction condition: T=220°C, P=300 psig, H_2/CO=2.0, SV=0.75 nL/h/g cat.).

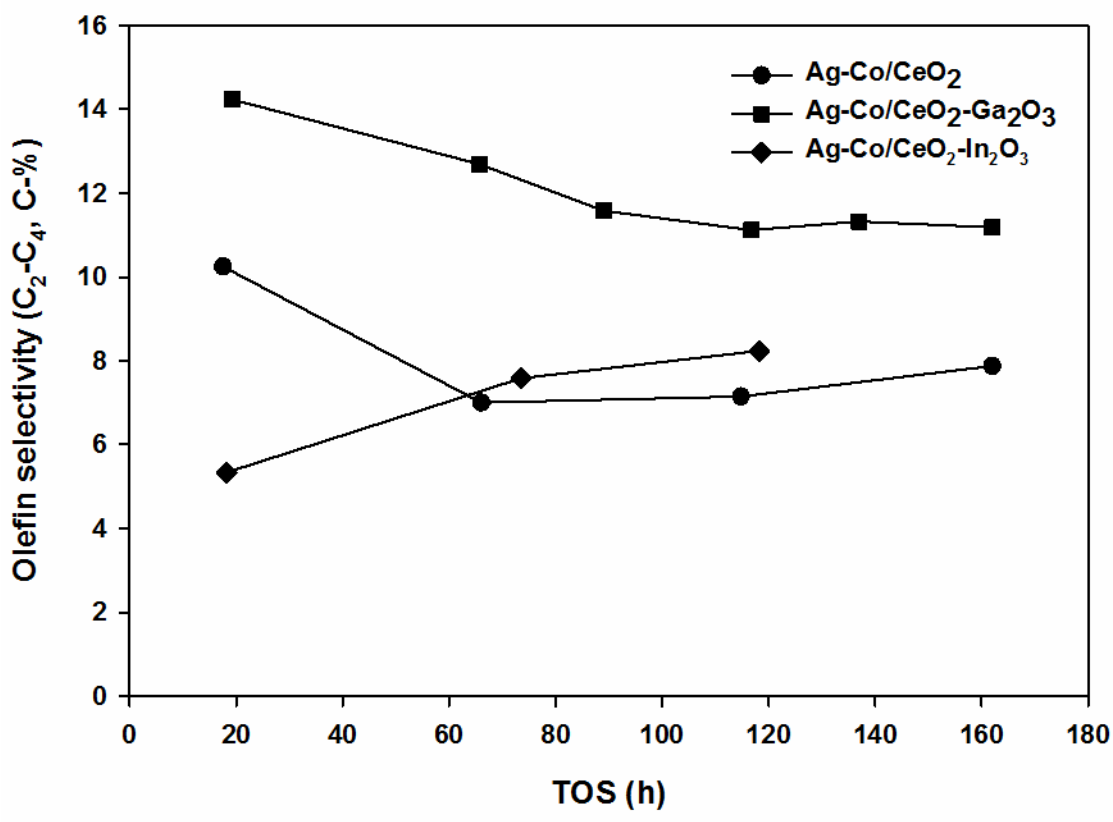

Figure 5. The lower olefins (C_2-C_4) selectivity as a function of time on-stream for FT synthesis over the Ag-promoted Co/Ce (Ce, Ce-Ga, Ce-In) catalysts. (Reaction condition: T=220°C, P=300 psig, H_2/CO=2.0, SV=0.75 nL/h/g cat.).

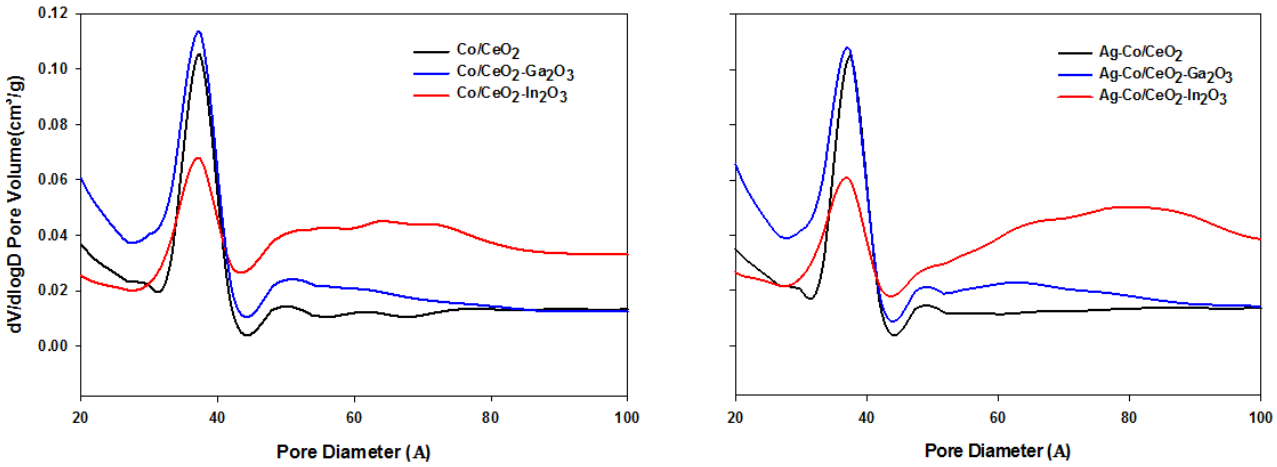

Figure 6. BJH pore size distributions (desorption branch) for the unpromoted (left) and Ag-promoted (right) Co/Ce (Ce, Ce-Ga, Ce-In) catalysts. (Reaction condition: T=220°C, P=300 psig, H_2/CO=2.0, SV=0.75 nL/h/g cat.).

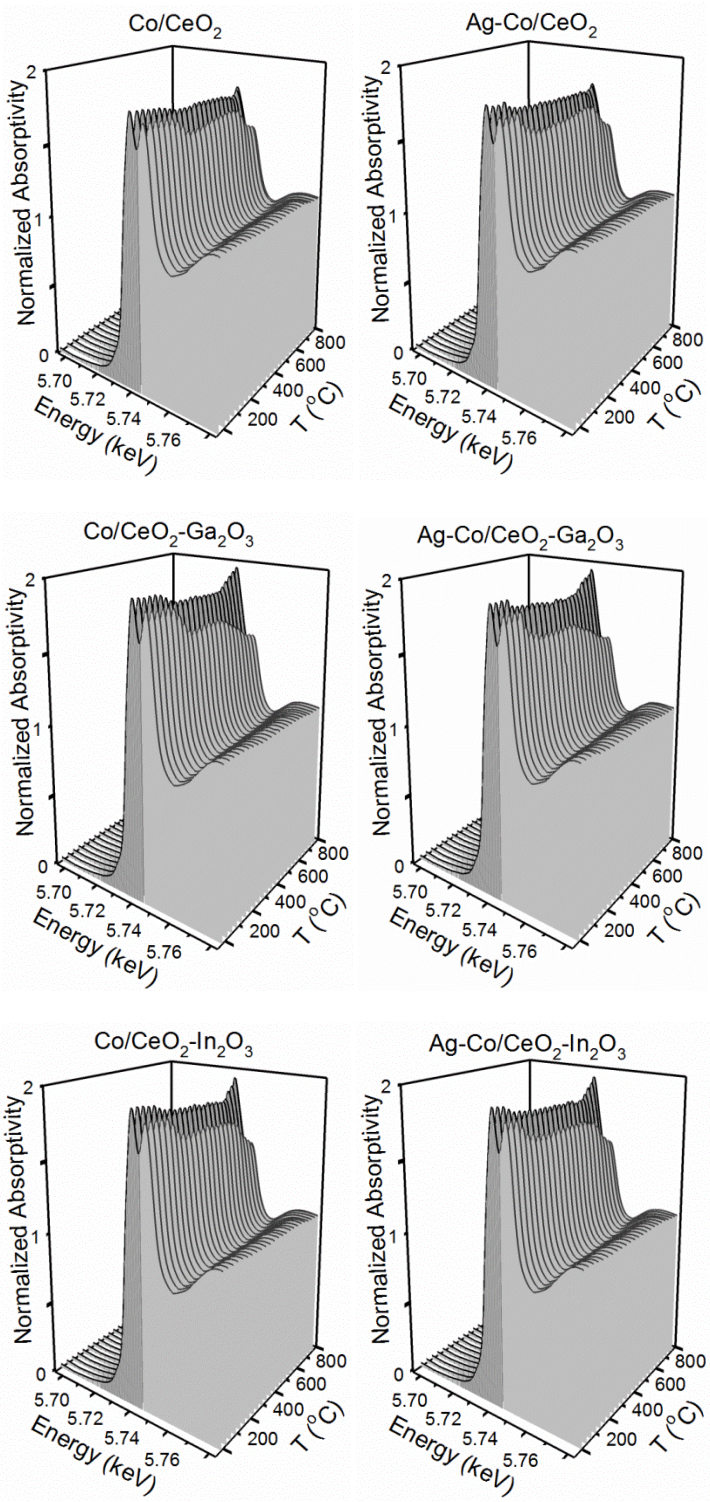

Figure 7. Hydrogen TPR-XANES profile for the unpromoted and Ag-promoted Co/Ce (Ce, Ce-Ga, Ce-In) catalysts as a function of temperature.

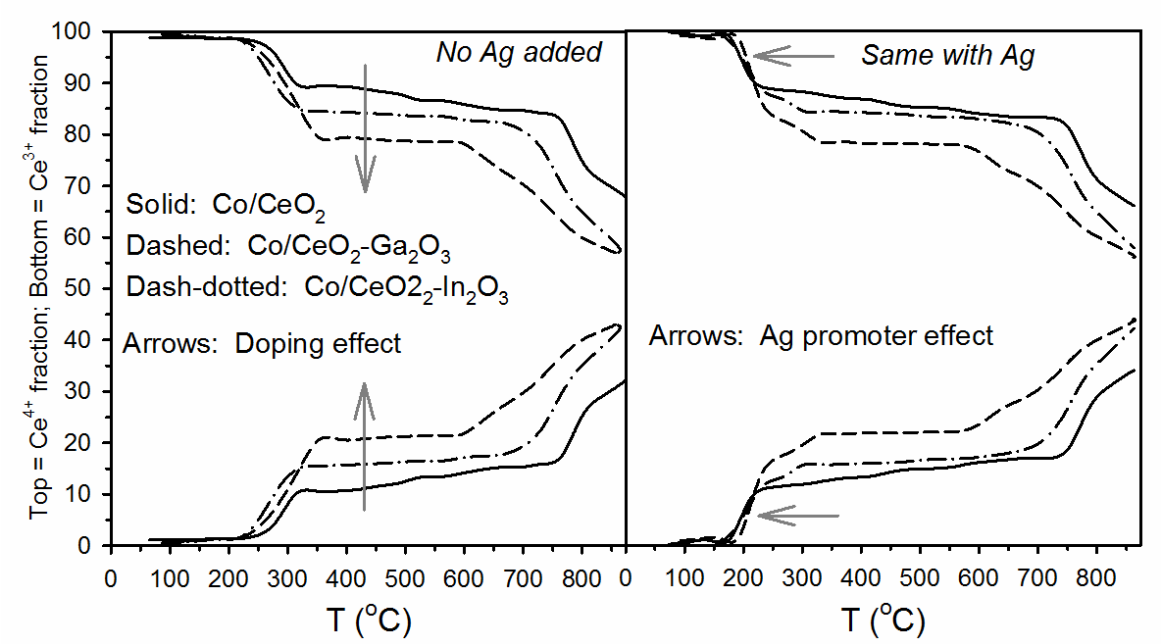

Figure 8. The percentage fraction of Ce^{4+} and Ce^{3+} found in the unpromoted and Ag-promoted Co/Ce (Ce, Ce-Ga, Ce-In) catalysts as a function of reduction temperature using H_2-TPR XANES.

(A)

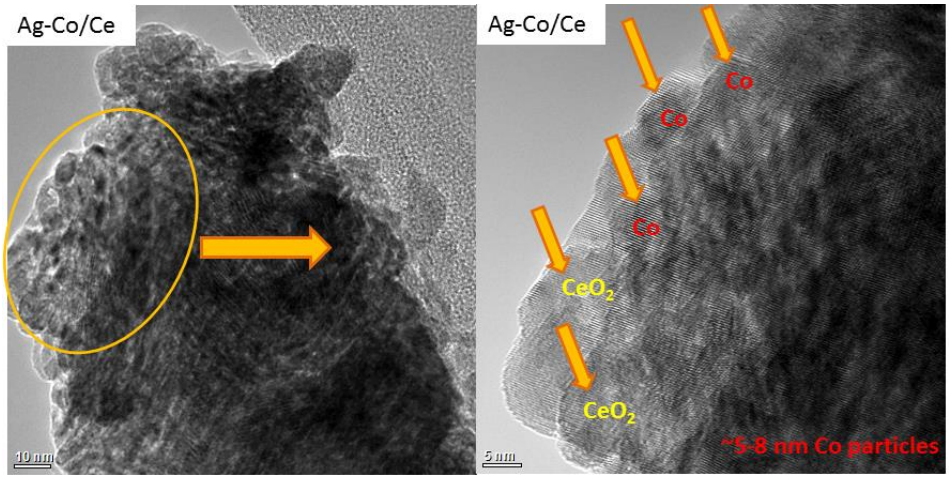
Ag-Co/Ce
Ag-Co/Ce
Co
Co
Co
CeO_2
CeO_2
~5-8 nm Co particles
10 nm
5 nm

(B)

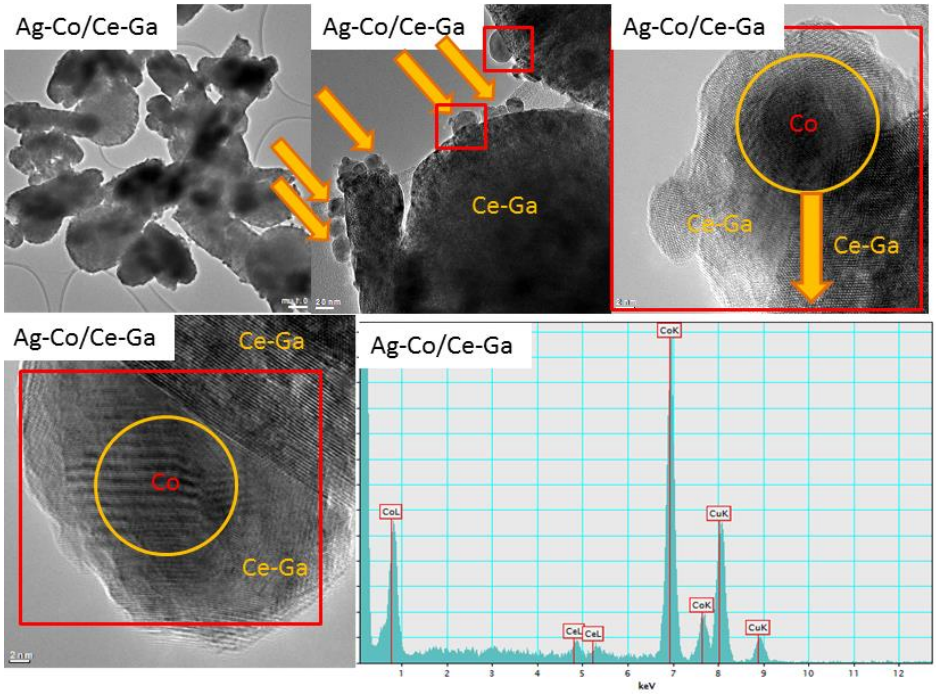
Ag-Co/Ce-Ga
Ag-Co/Ce-Ga
Ce-Ga
Ag-Co/Ce-Ga
Co
Ce-Ga
Ce-Ga
Ag-Co/Ce-Ga
Ce-Ga
Co
Ce-Ga
Ag-Co/Ce-Ga
CoK
CoL
CuK
CeL
CeL
CoK
CuK
keV

(C)

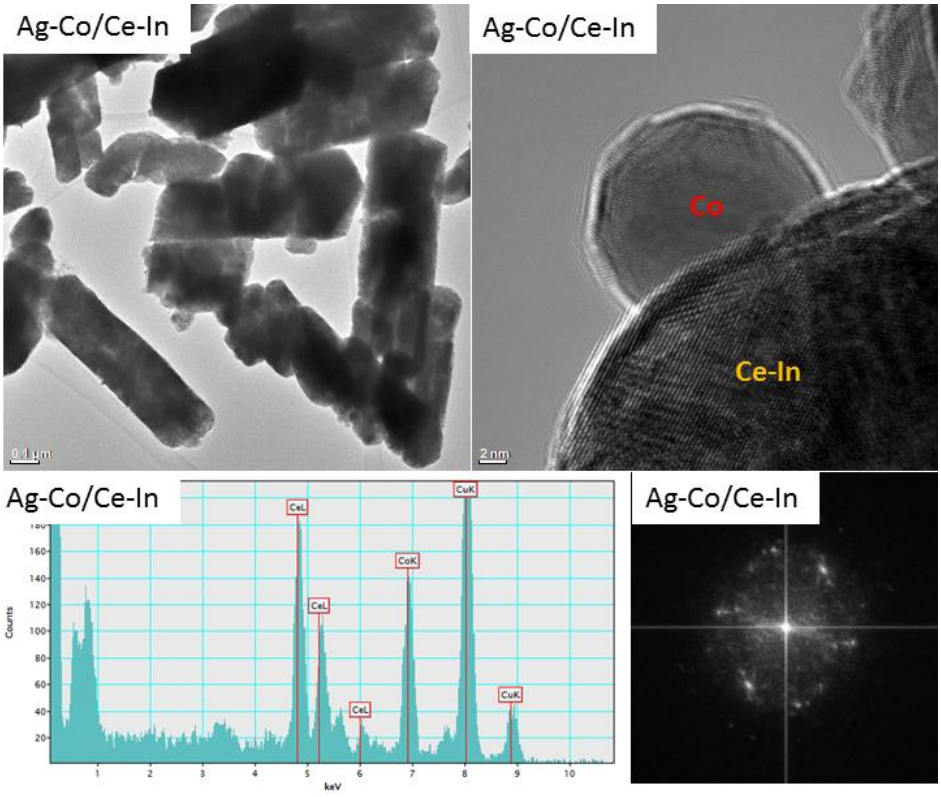

Figure 9. HRTEM images of the reduced sample of Ag-Co/Ce (A), Ag-Co/Ce-Ga (B), and Ag-Co/Ce-In (C).

Table 1 BET surface area and porosity measurements.

Catalyst	BET SA (m^2/g)	Single Point Pore Volume (cm^3/g)	BJH Des. Pore Volume (cm^3/g)	Single Point Pore Dia. (nm)	BJH Des. Pore Dia. (nm)
Ce	90	0.075	0.039	3.3	7.0
Ce-Ga	104	0.089	0.060	3.4	5.0
Ce-In	79	0.080	0.056	4.0	6.5
Co/Ce	71	0.062	0.039	3.5	5.6
Co/Ce-Ga	84	0.076	0.053	3.6	5.2
Co/Ce-In	61	0.068	0.053	4.4	6.7
Ag-Co/Ce	69	0.061	0.038	3.5	5.6
Ag-Co/Ce-Ga	88	0.080	0.057	3.7	5.3
Ag-Co/Ce-In	56	0.068	0.054	4.8	7.0

Table 2 Results of EXAFS fitting for data acquired near the Ce K-edge for samples treated in a H_2 flow at two different temperatures.

Sample Description	T (°C)	N Ce-O	% Decrease from Initial	R Ce-O (Å)	e_0 (eV)	σ^2 (Å^2)	r-factor
Co/Ce	25°C	4.87 (0.41)	-	2.295 (0.013)	5.46 (0.792)	0.00498 (0.00227)	0.0096
Ag-Co/Ce							
Co/Ce	275°C	4.80 (0.34)	-1.4%	2.297 (0.011)	6.60 (0.629)	0.00723 (0.00194)	0.0044
Ag-Co/Ce		4.50 (0.33)	-7.6%	2.300 (0.011)			
Co/Ce-Ga	25°C	5.21 (0.45)	-	2.300 (0.014)	5.81 (0.812)	0.00570 (0.00238)	0.0097
Ag-Co/Ce-Ga							
Co/Ce-Ga	275°C	5.11 (0.40)	-1.9%	2.306 (0.012)	6.27 (0.694)	0.00763 (0.00214)	0.0051
Ag-Co/Ce-Ga		4.70 (0.37)	-9.8%	2.289 (0.012)			
Co/Ce-In	25°C	5.28 (0.43)	-	2.301 (0.013)	5.85 (0.762)	0.00529 (0.00222)	0.0088
Ag-Co/Ce-In							
Co/Ce-In	275°C	5.18 (0.46)	-1.9%	2.303 (0.014)	6.40 (0.779)	0.00759 (0.00242)	0.0068
Ag-Co/Ce-In		4.77 (0.43)	-9.7%	2.306 (0.014)			